[24] Harris, F. D. and Pruyn, R. R., "Blade Stall. Half Fact, Half Fiction," *Journal of the American Helicopter Society*, Vol. 13, No. 2, April 1968, pp. 27–48.
[25] Garrick, I. E., "On Some Fourier Transforms in the Theory of Non-Stationary Flows," *Proceedings of the Fifth International Congress on Applied Mechanics*, Wiley, New York, 1938, pp. 590–593.
[26] Olsen, J. H., private communication, Nov. 1971, Flow Research Corp., Kent, Wash.

AUGUST 1973 AIAA JOURNAL VOL. 11, NO. 8

Hypersonic Wake Aerodynamics at High Reynolds Numbers

MICHAEL L. FINSON*
Avco Everett Research Laboratory Inc., Everett, Mass.

Motivated by ballistic range shadowgraphs, a theory has been developed for the wakes of slender cones under hypersonic, turbulent boundary-layer conditions. In the proposed model, the near wake is dominated by residual boundary-layer turbulence. It is shown that the intensity and scale size of this turbulence should be considerably smaller than equilibrium wake turbulence values. The resulting low-eddy viscosity provides an explanation for the slow observed wake growth. An approximate method is formulated for computing the near wake development of the turbulent intensities, Reynolds stress, and macroscale. Calculations in the expansion region suggest that a necessary condition for the postulated dominance of the near wake by residual boundary-layer turbulence is that the Reynolds number be sufficiently large that the boundary-layer turbulence not "relaminarize" upon expansion. The eventual recovery to equilibrium wake turbulence is predicted to require downstream distances of many hundreds of body diameters. Computed wake growth rates compare favorably with shadowgraph data.

I. Introduction

At moderate Reynolds numbers, the boundary layer on a body moving at hypersonic speeds is laminar and transition to turbulence occurs in the wake. Some time ago Lees and Hromas[1] showed that, downstream of the transition zone, the wake grows in a manner which may be described well by calculations based on a locally similar turbulent mixing rate. Recent ballistic range shadowgraphs have suggested a very different wake behavior at higher Reynolds numbers, where there is a well-developed turbulent boundary layer on the body. As an example, Fig. 1 shows shadowgraphs of the near wakes of two cone launchings carried out at the Naval Ordnance Lab.[2] For the case shown in the upper photograph, at $M_\infty = 6.3$, the boundary layer is laminar. Due to the relatively high Reynolds number in this laminar case ($Re_{\infty,D} = 3 \times 10^6$), there is no noticeable laminar run in the wake. Transition occurs in the neck region, and seems to cause a rapid establishment of large scaled, intense wake turbulence. In the lower photograph the boundary layer is clearly turbulent. Although it must be recognized that shadowgraphs can provide distorted impressions of the flow (they respond to the second derivative of the density, and may observe only the outer portions of the wake), there appears to be a distinct difference in flow structure between the two cases. This difference was first noticed by Levensteins and Krumins[3] in their analysis of these and many other shadowgraphs. Both the standard deviation and the correlation microscale of the wake edge location were found to be significantly smaller in the turbulent boundary-layer case. They noted that "It appears that the scale of turbulence that exists in the turbulent boundary layer persists for some distance downstream in the wake. Subsequently, a transition to larger-scale turbulence occurs. For the flow

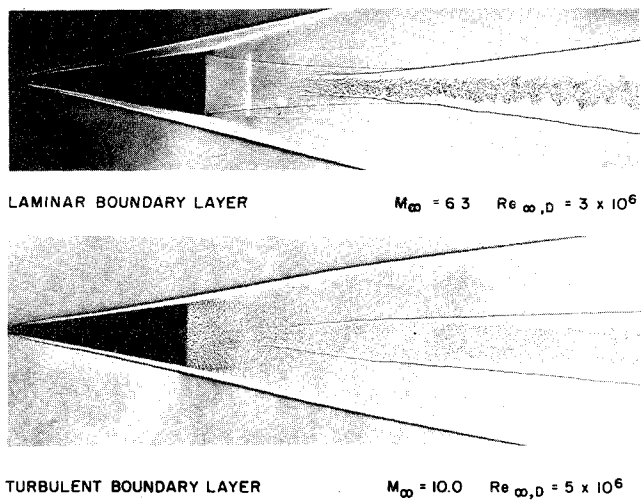

Fig. 1 Naval Ordnance Lab. ballistic range shadowgraphs[2] of typical laminar and turbulent boundary-layer cases.

Presented as Paper 72-701 at the AIAA 5th Fluid and Plasma Dynamics Conference, Boston, Mass., June 26–28, 1972; submitted September 1, 1972; revision received February 26, 1973. This work was supported by the U.S. Army, Advanced Ballistic Missile Defense Agency, under contract DAHC 60-69-C-0013.
Index categories: Jets, Wakes, and Viscid-Inviscid Flow Interactions; Supersonic and Hypersonic Flow; Viscous Nonboundary Layer Flows.
* Principal Research Scientist. Member AIAA.

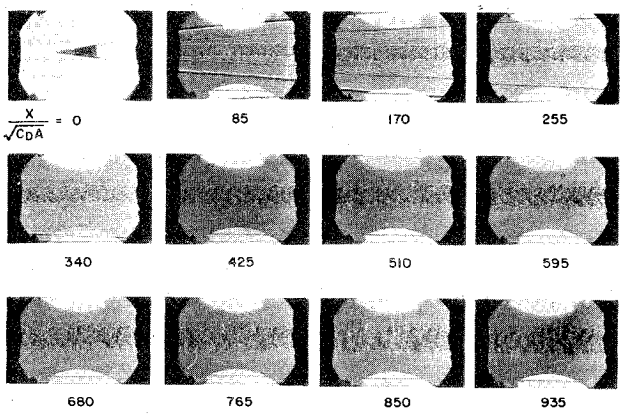

Fig. 2 Delco ballistic range shadowgraphs[4] for a nearly sharp 8° graphite cone at $M_\infty = 20$.

condition shown ..., it occurs at approximately 80 body diam downstream."

Figure 2 shows a series of sequential shadowgraphs taken in the Delco ballistic range.[4] In this case the model is a nearly sharp, nonablating, 8° cone flying at $M_\infty \cong 20$ and $Re_{\infty,D} \cong 7 \times 10^6$. The filming rate was such that the distance from the middle of one photograph to the middle of the next is about 17 body diam or $\approx 85(C_D A)^{1/2}$'s. (For a sharp 8° cone, typical of nearly all the cases to be considered here, $C_D \cong 0.06$ and the drag diameter $(C_D A)^{1/2}$ is about $0.2D$.) The photographs are mounted closer together in Fig. 2 for the sake of clarity. Here again there is the suggestion that boundary-layer turbulence flows off the body and dominates the near wake. The more familiar large-scale wake structure eventually appears, but only after distances on the order of $10^3(C_D A)^{1/2}$.

A better measure of the difference between the laminar and turbulent boundary-layer cases is provided by the rate of growth of the turbulent wake width. This is illustrated by Fig. 3, where we have plotted the average turbulent wake radius vs downstream distance. The data[5] were measured from Delco ballistic range shadowgraphs for sharp 8° cones fired at $M_\infty = 20$. The case with the turbulent boundary layer is the one already shown in Fig. 2. For the laminar case ($Re_{\infty,D} = 1.4 \times 10^6$) the data have been plotted from the observed transition location, which was about 10 diam behind the body. For each case, a computation based on the Lees-Hromas theory[1] is shown for comparison. The key feature of this theory is that it uses an integral method of solution, with the wake growth based on the eddy viscosity appropriate to equilibrium wake turbulence (proportional to the wake width and the mean velocity difference across the wake). At the initial station, the mass flux contained in the wake is presumed to equal the boundary-layer mass flux.

There are two obvious differences between the two cases. First, the wake is initially wider when the boundary layer is turbulent, reflecting the greater mass flux in the turbulent boundary layer. Second, the wake growth rates are not the same. With the laminar boundary layer, the wake is observed to grow right from the transition location, approximately obeying the asymptotic $x^{1/3}$ law. The theory shows a similar growth, although the computed values are consistently $\sim 25\%$ less than those observed. This mild difference probably results from the manner in which the wake radius is defined. (The computed wake radius is identified with the location of 50% intermittency, which could easily be less than that corresponding to the average apparent interface location on a shadowgraph.) In the case with the turbulent boundary layer the data show an almost negligible growth rate for several hundred $(C_D A)^{1/2}$'s. Here the theory significantly overpredicts the observed wake growth. Furthermore, it is hard to imagine how any modification which might be introduced to improve the comparison in the laminar boundary-layer case would not help but worsen the comparison in the turbulent case.

The significance of these comparisons should not be underestimated. Such quantities as wake temperature excess, velocity deficit, or concentration of a contaminant species all vary as r_w^{-2}, to a first approximation. No data reflecting any of these quantities are presently available from these ballistic range tests. However, we would expect that the decay rate of such quantities would be more seriously overpredicted than is the wake growth in the turbulent boundary-layer case.

II. High Reynolds Number Wake Model

The comparisons of Fig. 3 have led us to formulate a wake theory for turbulent boundary-layer conditions that departs significantly from the Lees-Hromas theory previously developed for cases with laminar boundary layers. Before arriving at the present model we investigated various modifications to the Lees-Hromas model. First, the possibility of inaccurate specification of the initial momentum deficit or of the wake front conditions was checked and discarded. We also evaluated the possibility of a very narrow initial turbulent wake. The idea here was that the shadowgraphs might be observing decaying turbulence on the outer boundary-layer streamlines, which would be dynamically unimportant but would shield an inner wake characterized by vigorous turbulence. This inner turbulence could be generated by the shear layer surrounding the base recirculation region or by an instability involving only streamlines very near the axis (in contrast to the laminar boundary-layer situation where wake transition seems to involve nearly all the flux from the boundary layer[1]). However, even if the initial radius were taken to be as small as 1/4–1/3 of the observed wake radius, the wake quickly ingested the streamlines from the outer portion of the boundary layer. Beyond $x/(C_D A)^{1/2} \cong 100$ these computations differed negligibly from those shown in Fig. 3. Since wake growth rates are proportional to turbulent mixing rates, the inescapable conclusion appeared to be that the near wake eddy viscosity must be much lower than the self-similar values inherent to the Lees-Hromas model.

The key feature of the model which we propose here for turbulent boundary-layer conditions is that the near wake is dominated by residual boundary-layer turbulence, convected from the trailing edge. This concept is consistent with the structure seen in Figs. 1 and 2 and, in fact, was first suggested by examination of those shadowgraphs. This residual boundary-

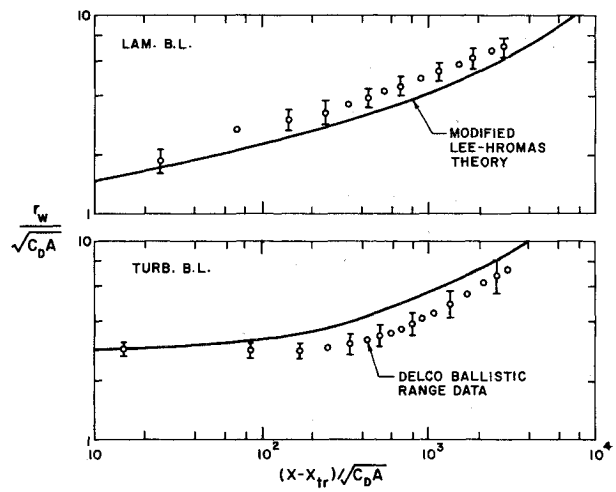

Fig. 3 Wake growth for sharp cones at $M_\infty = 20$ for laminar and turbulent boundary-layer conditions—comparison of Delco ballistic range data and Lees-Hromas theory.[1]

layer turbulence is characterized by lower intensities (i.e., rms fluctuating velocity $\hat{u}$) and smaller scale sizes (turbulence macroscale Λ) than would be equilibrium wake turbulence. Correspondingly, the eddy viscosity is relatively low, explaining the low growth rate observed in the near wake. Description of the downstream behavior requires computation of the relaxation of the turbulence toward equilibrium wake turbulence. As a final aspect of the model, it is postulated that the residual boundary-layer turbulence prevents the amplification of large scale instabilities.

We may illustrate the nature of near wake turbulence by accounting for the effect of the rapid trailing edge expansion on boundary-layer turbulence. In so doing we shall neglect the production and dissipation of turbulence energy and tacitly assume that the turbulence remains nearly isotropic. These estimates will not necessarily be self-consistent since dissipation and the tendency towards isotropy proceed at similar rates. However, we desire only estimates here, and more detailed results will be presented below. Pirri's analysis[6] may be interpreted to indicate that, in the present level of approximation, the average value of the rms fluctuating velocity $\hat{u}$ should vary as $\rho^{1/3}$ in an expanding flow. Similarly, the macroscale Λ varies as $\rho^{-1/3}$. To first order, the density ρ goes as $p^{1/\gamma}$ during the expansion (isentropic flow). Since the cone pressure is about 15 times the ambient pressure for an 8° cone at $M_\infty = 20$, the factor $\rho^{1/3}$ changes by about 2. To specify the trailing edge boundary-layer properties, we may refer to the recent hot wire measurements of Laderman and Demetriades[7] in a cold-wall boundary layer at $M_e \cong 10$. This edge Mach number is appropriate to an 8° cone at $M_\infty = 20$. They measured rms velocity fluctuations of about 2% of the edge velocity, and scale sizes about 20% of the boundary-layer thickness δ. For cases of interest, $\delta \cong 0.05R_b$ and $u_e \cong u_\infty$. Combining these numbers, the estimated state of the expanded boundary-layer turbulence in the near wake (say, immediately downstream of the neck) is

$$\hat{u}/u_\infty \sim 0.02/2 \sim 0.01, \quad \Lambda/R_b \sim (0.2)(0.05)(2) \sim 0.02 \qquad (1)$$

By way of comparison, equilibrium wake turbulence has been well measured[8-10] (at least at subsonic and moderately supersonic speeds) to be characterized by fluctuating velocities equal to about 40% of the mean velocity difference across the wake ($\Delta\bar{u}$) and macroscales about 15% of the wake radius. The calculations performed for Fig. 3 indicate that $\Delta\bar{u} \sim 0.2u_\infty$ and $r_w \sim R_b$ in the near wake. Thus equilibrium wake turbulence would be described by

$$\hat{u}/u_\infty \sim (0.4)(0.2) \sim 0.08, \quad \Lambda/R_b \sim 0.15 \qquad (2)$$

in the near wake. Comparison of Eqs. (1) and (2) shows that the intensity and scale size of the residual boundary-layer turbulence are both nearly an order of magnitude below the equilibrium wake turbulence values. Furthermore, since eddy viscosities are usually roughtly proportional to the product $\hat{u}\Lambda$,[11] the near wake mixing rate is reduced by nearly two orders of magnitude in comparison to equilibrium wakes.

One feature of the near wake flow which is neglected in the proposed model is the free shear layer surrounding the base recirculation region. The free shear layer contains only a small fraction of the boundary-layer streamlines but could have an important influence if large turbulent intensities were to be generated on the innermost streamlines. There are two reasons why we do not feel that this occurs. First, as already mentioned, an initially narrow zone of intense turbulence will grow rapidly and fail to explain the observed wake growth. Second, it is doubtful that the shear layer could generate turbulent intensities much larger than the value quoted in Eq. (1). Turbulent production (means shear times the turbulent stress) would not yield an intensity much greater than a boundary-layer value ($\hat{u}/u_\infty \sim 0.02$), since the shear is no greater in the shear layer than in the boundary layer. If the shear layer were unstable, there might be an "overshoot" to slightly higher intensities. However, it is well-known that hypersonic shear layers are remarkably stable, at least in laminar flows (see, e.g., Ref. 12).

Stabilization of the near wake by residual boundary-layer turbulence is one aspect of the model that does not explicitly enter the calculations presented in the following sections. However, this stabilization must be mentioned. In the absence of the residual boundary-layer turbulence the near wake would surely be inviscidly unstable, with the result that relatively vigorous, large-scaled turbulence would quickly be established in a manner similar to that observed in laminar boundary-layer cases at moderately high Reynolds numbers. Lacking a better understanding of the nonlinear interaction between fluctuations of different wavelengths—a fundamental problem in turbulence modeling—we must offer this postulate without proof. It is clear that the fine-scaled nature of the background turbulence is important, for large eddies would serve merely as initial disturbances. Crow[13] has described the complexity of the interaction between a disturbance and background turbulence. He showed that the turbulence acts in a visco-elastic manner, and that the effects of inertia, dissipation, shear, etc. must all be considered to determine the stresses acting on the disturbance. Although not well understood, the concept of background turbulence playing a damping role is not new. Crow and Champagne[14] mentioned fine-scaled turbulence as a possible mechanism for damping and orderly structure observed in turbulent jets. Roshko's measurements[15] showed turbulence to be extremely effective for destroying the large vortices in the vortex street behind a cylinder. Also, reduced ocean wave activity in the wakes of ships is a common observation which could be explained in terms of fine-scaled turbulence.

Finally, we might note the discussion by Bradshaw and Wong[16] of the behavior of boundary-layer turbulence downstream of steps and fences. They proposed three classifications for the strength of the perturbation that can be applied to an initially thin shear layer: weak, where only the mean flow structure is perturbed; strong, where the turbulent structure is altered significantly; and overwhelming, where the flow changes to one of a different species, "as in the mutation of a boundary layer into a wake or mixing layer." The latter two categories involve nonsimilar or nonequilibrium turbulence behavior, and the problem considered here would obviously fall into the third category.

III. Turbulence Conservation Equations

The ability to describe the behavior of high Reynolds number wakes hinges on the determination of the nonsimilar development of turbulence downstream of the trailing edge. In this section we will develop a set of governing equations for the relevant turbulence parameters. These equations will first be used to improve upon the estimates presented above for the effect of the trailing edge expansion upon boundary-layer turbulence. Then, an integral method will be used to track the development of wake turbulence downstream of the neck. From the low near wake values, we may anticipate that turbulent intensities will increase due to production of turbulent energy by mean shear work, and the scale size will be increased by dissipation. Eventually, these processes will result in the establishment of equilibrium wake turbulence. A primary objective is to estimate the required distance for this relaxation.

The present formulation has profited greatly from the pioneering work of Rotta.[17] As proposed by Rotta, it is necessary to compute the usual mean flow properties plus five "second-order" turbulence parameters: the three components of the mean square fluctuating velocity, the Reynolds stress, and the scale size. The motivation for this set of variables will be made more clear below. Donaldson,[18] Harlow,[19] Launder,[20] and their respective co-workers have developed formulations similar to that presented here.

The governing equation for a component of the Reynolds stress tensor $\overline{u_i'u_j'}$ can be derived from the Navier-Stokes equation. To do this, one has to multiply the momentum equation in the i direction by u_j', add the corresponding equation with i and j reversed, and then average. The result, for steady flow, is

$$\bar{\rho}\bar{u}_k \overset{(1)}{\frac{\partial}{\partial x_k}}(\overline{u_i'u_j'}) = -\left[\bar{\rho}\,\overline{u_k'u_j'}\,\frac{\partial \bar{u}_i}{\partial x_k} + \overset{(2)}{\bar{\rho}\,\overline{u_k'u_i'}\,\frac{\partial \bar{u}_j}{\delta x_k}}\right] -$$

$$\frac{\partial}{\partial x_k}\underset{(3a)}{[\bar{\rho}\,\overline{u_k'u_i'u_j'}} + \underset{(3b)}{\bar{u}_k\overline{\rho'u_i'u_j'}} + \underset{(3c)}{\overline{\rho'u_k'u_i'u_j'}}] -$$

$$\left[\overset{(4)}{\overline{\rho'u_j'}\,\bar{u}_k\frac{\partial \bar{u}_i}{\partial x_k}} + \overline{\rho'u_i'}\,\bar{u}_k\frac{\partial \bar{u}_j}{\partial x_k}\right] + \overset{(5)}{\overline{u_i'u_j'}\,\frac{\partial}{\partial x_k}(\overline{\rho'u_k'})} -$$

$$\left[\overset{(6)}{\overline{\rho'u_k'u_j'}\,\frac{\partial \bar{u}_i}{\partial x_k}} + \overline{\rho'u_k'u_i'}\,\frac{\partial \bar{u}_j}{\partial x_k}\right] -$$

$$\left[\overset{(7)}{\frac{\partial}{\partial x_j}(\overline{u_i'p'}) + \frac{\partial}{\partial x_i}(\overline{u_j'p'})}\right] + \left[\overset{(8)}{\overline{p'\frac{\partial u_i'}{\partial x_j}} + \overline{p'\frac{\partial u_j'}{\partial x_i}}}\right] +$$

$$\mu\left[\overset{(9)}{\nabla^2\overline{u_i'u_j'}} - 2\overset{(10)}{\overline{\frac{\partial u_i'}{\partial x_k}\frac{\partial u_j'}{\partial x_k}}}\right] \qquad (3)$$

Summation over k is implied. The following interpretation is generally attached to the various terms in this equation: term (1) is convection, term (2) is production, terms (3) and (7) represent turbulent diffusion, terms (4–6) contain compressibility effects, term (8) drives the flow toward isotropy, term (9) is molecular diffusion, and term (10) is dissipation. The governing equation for the scale size is derived in the Appendix and will be presented below.

Equation (3) illustrates the fundamental difficulty in describing turbulent flows. The equation contains additional unknown statistical quantities—in the turbulent diffusion, pressure fluctuation, density fluctuation, and dissipation terms. Closure approximations must be introduced for these terms, and that is a formidable task which places great demands on the present understanding of turbulent free shear flows. The approximations which we shall introduce are due mainly to Rotta.[17]

The first terms to be addressed in Eq. (3) are the compressibility terms—those involving ρ'. We shall handle these terms by simply omitting them. It should be stressed that this approach cannot be defended adequately and is largely motivated by our inability to develop well-founded descriptions for such terms. However, estimates can be made to provide some justification for neglecting the ρ' terms. Of course, there is no problem in the far wake where $\rho'/\bar{\rho} \to 0$. For the residual boundary-layer turbulence in the near wake, the rms density fluctuations are

$$\hat{\rho}/\bar{\rho} \sim 0.1 - 0.2 \qquad (4)$$

This value may be obtained in two ways. By analogy with the velocity fluctuations the rms density should be about a factor of eight below the equilibrium value, which would be $\hat{\rho} \sim 0.4\Delta\bar{\rho}$; for an 8° cone at $M_\infty = 20$, $\Delta\bar{\rho} \lesssim 3\bar{\rho}$. Alternatively one could equate $\hat{\rho}/\bar{\rho}$ to $\hat{T}/\bar{T}$ in the boundary layer ($\hat{T}/\bar{T} \sim 0.1^7$), and assume eddies to be frozen during the expansion. With Eq. (4) it may be claimed that term (6) in Eq. (3) should be smaller than term (2) by a factor on the order of 5–10. Similarly term (3c) should be smaller than term (3a), and term (5) must be very small. Term (4) is found to be negligible if the boundary-layer approximations are applied to the mean flow. On the other hand, term (3b) cannot be shown to be small compared to term (3a). This is probably not too serious since terms (3) and (7) are generally grouped together in a single turbulent diffusion term, and the main concern here is with processes that create and destroy turbulence. Thus there is some rationale for neglecting the effects of compressibility in the near wake. That is not to say there might not be some intermediate downstream stations where they are important, and the present approach must be regarded as a first approximation.

For the dissipation term (10) we follow Rotta and others:

$$\mu\overline{\frac{\partial u_i'}{\partial x_k}\frac{\partial u_j'}{\partial x_k}} = \frac{k_d}{3}\bar{\rho}\frac{E^{3/2}}{\Lambda}\delta_{ij} + \frac{5\pi}{2}\mu\frac{\overline{u_i'u_j'}}{\Lambda^2} \qquad (5)$$

where E is the turbulent kinetic energy $u_k'u_k'/2$. The first term applies to high turbulence Reynolds numbers ($Re_\Lambda = (E)^{1/2}\Lambda/\nu$). In this limit there should be a large separation between energy-containing scales and dissipation scales and the turbulence should be essentially isotropic at the small scales, hence there is no such dissipation term for the Reynolds stress ($i \neq j$).[17] The constant k_d is presumed to be universal. The final term in Eq. (5) applies for small turbulence Reynolds numbers. In the limit $Re_\Lambda \to 0$ the Navier-Stokes equations are linear and these terms are exact solutions which were derived by Batchelor and Townsend.[21]

The pressure fluctuation term (8) drives the turbulence toward isotropy (strictly true only for incompressible turbulence). Here we also follow Rotta's suggestions. It is more convenient to specialize the result to the coordinates to be used below

$$\overline{p'\frac{\partial u_i'}{\partial x_i}} = -\frac{k_p}{2}\bar{\rho}\frac{(E)^{1/2}}{\Lambda}(u_i'u_i' - \tfrac{2}{3}E) + a_i\bar{\rho}\,u_1'u_2'\frac{\partial \bar{u}_1}{\partial x_2} \qquad (6a)$$

$$\overline{p'\left(\frac{\partial u_i'}{\partial x_j} + \frac{\partial u_j'}{\partial x_i}\right)} = -k_p\bar{\rho}\frac{(E)^{1/2}}{\Lambda}\overline{u_i'u_j'} + b_1\bar{\rho}\,\overline{u_2'u_2'}\frac{\partial \bar{u}_1}{\partial x_2} \qquad (6b)$$

[no summation over i in Eq. (6a)]. The first terms on the right side are the ones which have often been used. The second terms result from an expansion using the Green's function for p';[17] third and higher derivatives of the mean velocity are neglected. Five new closure constants are introduced in Eq. (6): k_p, a_1, a_2, a_3, b_1, but continuity requires that $a_1 + a_2 + a_3 = 0$. Finally, the turbulent diffusion terms (3) and (8) are generally modeled by gradient diffusion with coefficients proportional to the eddy viscosity. The constants of proportionality become additional "closure" constants. However, they will not be discussed in detail since the computations of Sec. IV are not fundamentally dependent upon them.

The formulation of the turbulence conservation equations is now complete except for determination of the various closure constants. There are seven of these, all of which are presumed to be universal: k_d, k_p, a_1, a_2, b_1, d_1, and d_2. The latter two represent spectral moments appearing in the scale size equation (see Appendix). Some recent investigators have chosen to evaluate the constants by comparing solutions with laboratory data in various fully developed flows: channels, jets, wakes, and boundary layers. We have adopted a somewhat different approach in that we have analyzed low-speed grid turbulence data. The analysis is best carried out in several stages, involving successively more complicated types of grid turbulence. This has the advantage of isolating the various terms, and should be admissible if the constants are indeed universal. We then checked that the values determined yield a reasonable solution for equilibrium wake turbulence.

The least complicated turbulent flow is the decay of isotropic, homogeneous turbulence. In this case the governing equations are those for the kinetic energy [contraction of Eq. (3)] and scale size. Only the convection and dissipation terms appear, involving the constants k_d and d_1. For high turbulence Reynolds numbers the equations admit analytical solutions in the form of power laws

$$E \sim x^{-1/(\frac{3}{2}-d_1)}, \quad \Lambda \sim x^{(1-d)/(\frac{3}{2}-d_1)} \qquad (7)$$

Comte-Bellot and Corrsin[22,23]† obtained a considerable quantity of data where special care was taken to establish isotropy. They found that their data and those of others gave

$$E \sim x^{-(1.25\pm0.05)}, \quad \Lambda \sim x^{(0.35-0.40)} \qquad (8)$$

Thus we establish $d_1 = 0.70 \pm 0.05$. Figure 4 shows a typical comparison with the Comte-Bellot and Corrsin data.[22] From the absolute values of E and Λ, the constant k_d is found to be 0.4 (with probably more than a few percent uncertainty due to inaccuracies in the measured Λ values). Dissipation rates determined from various experiments[21–26] are compared with Eq. (5) in Fig. 5. We have called attention to the range Re_Λ = 10–30,

† The author is indebted to Prof. Corrsin for making a copy of Ref. 23 available prior to its publication.

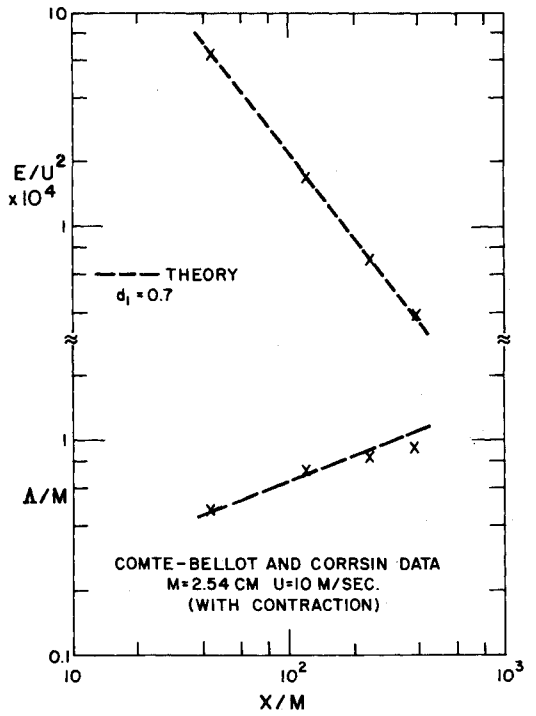

Fig. 4 Comparison of calculated decay of turbulent kinetic energy and growth of macroscale with the low-speed grid turbulence measurements of Comte-Bellot and Corrsin.[22,23]

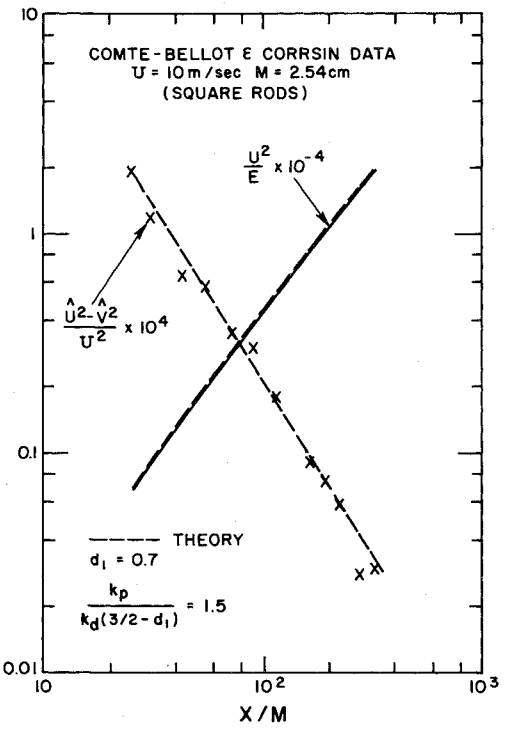

Fig. 6 Comparison of calculated decay of turbulent kinetic energy and approach toward isotropy with the low-speed grid turbulence measurements of Comte-Bellot and Corrsin.[22,23]

which may be thought to separate the high- and low-turbulence Reynolds number regimes: any value for Re_Λ much below 10 certainly corresponds to low Reynolds number turbulence, while the dissipation rate is within a factor of two of the infinite Reynolds number limit for $Re_\Lambda > 30$.

Next, there are data involving anisotropic homogeneous grid turbulence, in which case the equations for the individual rms fluctuations are required and the pressure-fluctuation term involving k_p enters. Analytical solutions can again be obtained:

$$(\hat{u}^2-\hat{v}^2)/U^2 \sim x^{-k_p/k_d(\frac{3}{2}-d_1)} \tag{9}$$

Comparison with numerous sets of data from Ref. 22, an example of which is shown in Fig. 6, indicates that $k_p/k_d(\frac{3}{2}-d_1) = 1.50 \pm 0.10$ or $k_p \cong 0.48$.

Finally, we analyzed data from grid turbulence experiments where there was a uniform mean shear.[27,28] This yields the other four constants. Comparison with the measurements of Champagne et al.[27] is presented in Fig. 7. The computations were matched to the data at the initial station. As noted, the comparison indicates that $a_1 = 0.4$, $a_2 = 0.125$, $b_1 = 0.675$, and $d_2 = 0.63$. Satisfactory agreement with Rose's data[28] was also obtained using these same values. However, the conditions for these two experiments are very similar, and additional tests at other values of the mean shear would be most useful.

We shall now write down the governing turbulence equations

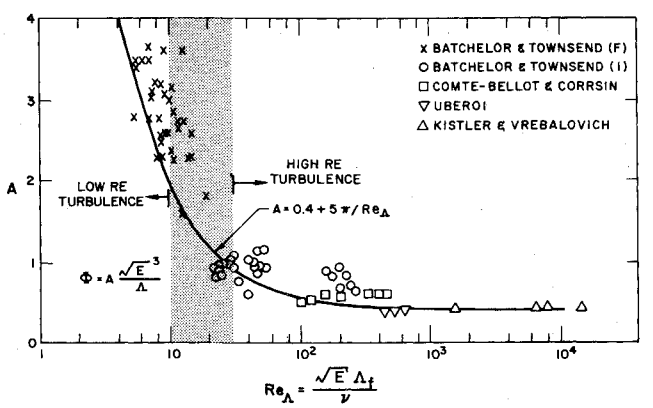

Fig. 5 Dissipation rate (Φ) in grid turbulence as a function of turbulent Reynolds number.

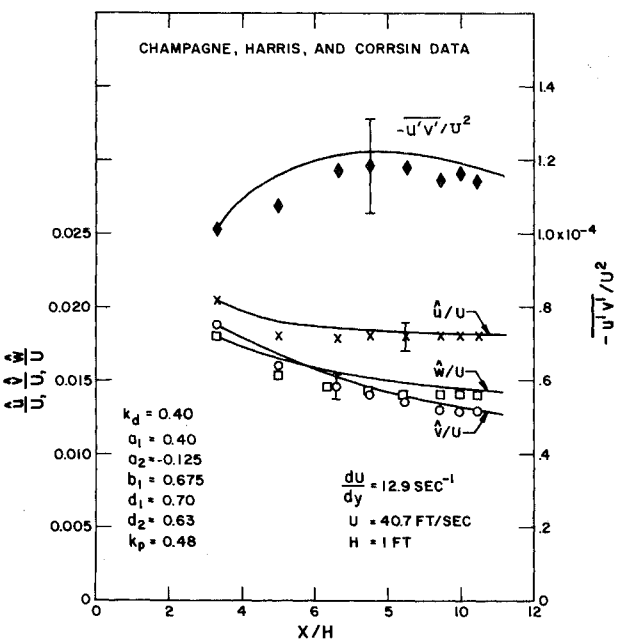

Fig. 7 Comparison of calculated downstream development of rms velocity fluctuations and Reynolds stress with the measurements of Champagne et al.[27] in grid turbulence with a uniform mean shear.

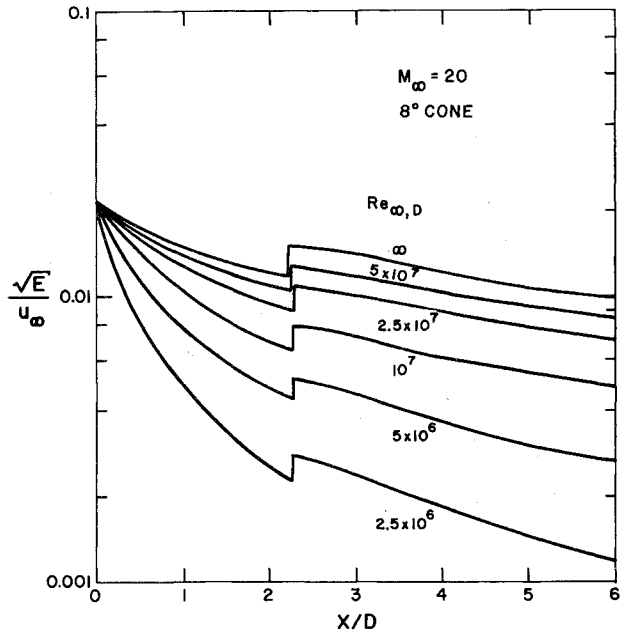

Fig. 8 Predicted turbulent intensity decay in the very near wake vs Reynolds number.

in cylindrical coordinates. The boundary-layer approximations ($\bar{u}_x \gg \bar{u}_r$, $\bar{u}_\theta$; $\partial/\partial r \gg \partial/\partial x$, $1/r\,\partial/\partial\theta$) may be applied in general although the term $\bar{\rho}\,\partial\bar{u}_r/\partial r$ should be retained. By continuity this term is approximately equal to $-\bar{u}\,\partial\bar{\rho}/\partial x$ and will be important during the expansion at the trailing edge. If we neglect the molecular diffusion terms,

$$\bar{\rho}\bar{u}\frac{\partial \hat{u}_x^2}{\partial x} = -2\bar{\rho}\,\overline{u_x'u_r'}\frac{\partial\bar{u}}{\partial r} - 0.48\bar{\rho}\frac{(E)^{1/2}}{\Lambda}(\hat{u}_x^2 - \tfrac{2}{3}E) + 0.8\bar{\rho}\,\overline{u_x'u_r'}\frac{\partial\bar{u}}{\partial r} - 0.267\bar{\rho}\frac{E^{3/2}}{\Lambda} - 5\pi\mu\frac{\hat{u}_x^2}{\Lambda^2} + \frac{1}{r}\frac{\partial}{\partial r}\left(\bar{\rho}\varepsilon_E r\frac{\partial \hat{u}_x^2}{\partial r}\right) \quad (10)$$

$$\bar{\rho}\bar{u}\frac{\partial \hat{u}_r^2}{\partial x} = 2\bar{u}\hat{u}_r^2\frac{\partial\bar{\rho}}{\partial x} - 0.48\bar{\rho}\frac{(E)^{1/2}}{\Lambda}(\hat{u}_r^2 - \tfrac{2}{3}E) - 0.25\bar{\rho}\,\overline{u_x'u_r'}\frac{\partial\bar{u}}{\partial r} - 0.267\bar{\rho}\frac{E^{3/2}}{\Lambda} - 5\pi\mu\frac{\hat{u}_r^2}{\Lambda^2} + \frac{1}{r}\frac{\partial}{\partial r}\left(\bar{\rho}\varepsilon_E r\frac{\partial \hat{u}_r^2}{\partial r}\right) \quad (11)$$

$$\bar{\rho}\bar{u}\frac{\partial \hat{u}_\theta^2}{\partial x} = -0.48\bar{\rho}\frac{(E)^{1/2}}{\Lambda}(\hat{u}_\theta^2 - \tfrac{2}{3}E) - 0.55\bar{\rho}\,\overline{u_x'u_r'}\frac{\partial\bar{u}}{\partial r} - 0.267\bar{\rho}\frac{E^{3/2}}{\Lambda} - 5\pi\mu\frac{\hat{u}_\theta^2}{\Lambda^2} + \frac{1}{r}\frac{\partial}{\partial r}\left(\rho\varepsilon_E r\frac{\partial \hat{u}_\theta^2}{\partial r}\right) \quad (12)$$

$$\bar{\rho}\bar{u}\frac{\partial\overline{u_x'u_r'}}{\partial x} = -\bar{\rho}\hat{u}_r^2\frac{\partial\bar{u}}{\partial r} + \bar{u}\,\overline{u_x'u_r'}\frac{\partial\bar{\rho}}{\partial x} - 0.48\bar{\rho}\frac{(E)^{1/2}}{\Lambda}\overline{u_x'u_r'} + 0.675\bar{\rho}\hat{u}_r^2\frac{\partial\bar{u}}{\partial r} - 5\pi\mu\frac{\overline{u_x'u_r'}}{\Lambda^2} + \frac{1}{r}\frac{\partial}{\partial r}\left(\rho\varepsilon_v r\frac{\partial\overline{u_x'u_r'}}{\partial r}\right) \quad (13)$$

$$\bar{\rho}\bar{u}\frac{\partial\Lambda}{\partial x} = 0.37\bar{\rho}\frac{\overline{u_x'u_r'}}{E}\frac{\partial\bar{u}}{\partial r}\Lambda + 0.12\bar{\rho}(E)^{1/2} + \frac{\pi\mu}{\Lambda} - \frac{1}{3}\bar{u}\Lambda\frac{\partial\bar{\rho}}{\partial x} \quad (14)$$

The form of the production terms shows why the Reynolds stress and the three mean square velocity fluctuations were selected as dependent variables. The Reynolds stress is the parameter of most interest since it is needed to determine the mean properties. However, production of $\overline{u_x'u_r'}$ involves $\hat{u}_r^2$, while only axial fluctuations are produced directly by the mean shear. Thus it is important to keep track of the various velocity components, as recognized by Rotta[17] and Donaldson and Rosenbaum.[18] But the latter authors introduced similarity approximations for the scale size, which clearly would not suffice for the present problem.

IV. Results

In this section the equations just formulated will be used to evaluate the behavior of high Reynolds number wake turbulence. First we will refine the foregoing estimates for the decay of turbulence in the expansion region, connecting the trailing edge and the region beyond the neck. Then the downstream wake development will be calculated for comparison with the ballistic range wake growth data.

To study the decay of the expanding boundary-layer turbulence, Eqs. (10–14) were integrated from the trailing edge through the recompression region. To keep the effort at a manageable level this integration was performed along a single streamline. The streamline position, as well as the distributions of density, temperature, and mean shear along the streamline, was obtained from a rotational method-of-characteristics calculation which was performed in the manner described in Ref. 29. We chose a streamline originating at $y/\delta = 1/6$, and ending up at $r/r_w \cong 0.4$ downstream of the neck (at, say, $x/D \gtrsim 5$). This streamline should be representative of inner boundary-layer streamlines. It coincides nearly with the peak boundary-layer turbulent intensity and peak temperature ($\sim$4000°K at $M_\infty = 20$); after expansion to p_∞ the temperature is $\sim$2000°K, typical of the inner portions of the near wake. Initial (trailing edge) conditions were taken from the boundary-layer measurements of Laderman and Demetriades[7,30] ($\hat{u}_x/u_\infty \cong 0.03$, $\hat{u}_r \cong 0.005$, $\hat{u}_\theta/u_\infty \cong 0.005$, $\Lambda/R_b \cong 0.0075$), and the eddy viscosity correlations of Maise and McDonald[31] ($\overline{u_x'u_r'}/u_\infty^2 = 0.0002$). Turbulent diffusion was neglected in the calculations because $\partial^2\bar{u}/\partial y^2$ becomes very small upon expansion.

Figure 8 shows the square root of the computed near wake turbulent kinetic energy. The initial decay ($x/D \lesssim 2$) is the result of expansion ($\partial\bar{\rho}/\partial x$) and dissipation. The sudden increase at $x/D = 2.2$ results from the density jump across the recompres-

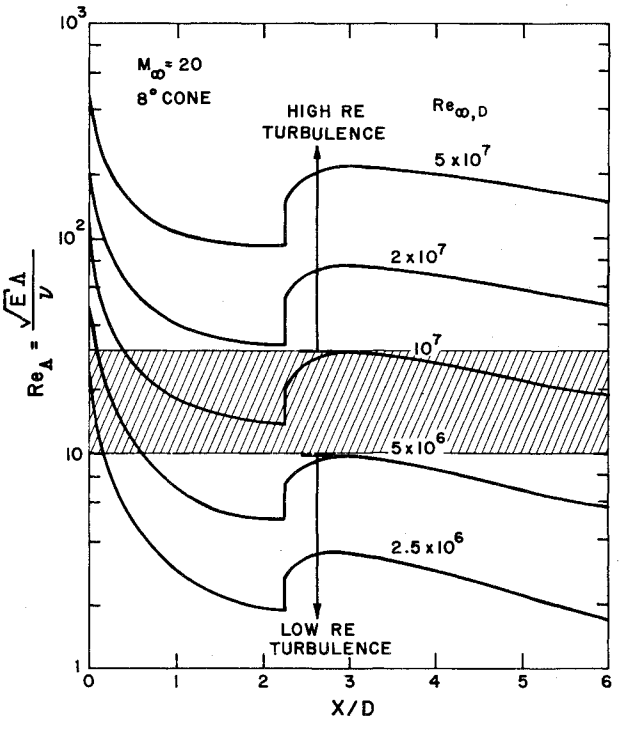

Fig. 9 Predicted near wake turbulence Reynolds numbers vs freestream Reynolds number.

sion shock. Dissipation causes the decay beyond $x/D \cong 4$. At large Reynolds numbers the results are seen to be consistent with the estimate given in Eq. (1) [$(E)^{1/2} = (3/2)^{1/2}\hat{u}$ for isotropic turbulence]. However, dissipation becomes far more important at low Reynolds numbers because of the increase in the final term in Eq. (5). The scale sizes are much less sensitive to Reynolds number and will not be shown here. The effect of expansion on the turbulence Reynolds number is described by Fig. 9. Note that Re_Λ is auite sensitive to $Re_{\infty,D}$, since $(E)^{1/2}$, Λ, and ν all vary with $Re_{\infty,D}$.

An interesting point here is the state of the residual boundary-layer turbulence at the lower Reynolds numbers. There the turbulent intensities become quite low. Moreover, since Re_Λ is roughly ε/ν, the eddy viscosity is not much greater than the molecular viscosity. It would seem reasonable to expect the turbulence to become dynamically unimportant at some minimum value of Re_Λ. In particular it could become too weak to provide the stabilization of the near wake postulated above. Inasmuch as the stabilization process is poorly understood we must be rather speculative at this stage, but we will state that the turbulence Reynolds number in the near wake (say, $x/D = 5$) must be greater than $\sim$10–30 for the high Reynolds number wake behavior to occur. That is, we are suggesting a more precise definition for what we mean by "high" Reynolds numbers: not only must the Reynolds number be sufficiently high for a well-developed turbulent boundary layer to exist on the body, it must also be high enough for the boundary-layer turbulence not to "relaminarize" upon expansion at the trailing edge.

To outline how this minimum Reynolds number requirement depends on Mach number, streamline calculations analogous to those just described were performed at various Mach numbers. Figure 10 shows the results, in terms of the freestream Reynolds numbers corresponding to $Re_\Lambda = 10$–30 in the near wake. The suggestion, of course, is that the high Reynolds number wake behavior would occur for conditions above the shaded areas but not below. It is necessary to distinguish between hot (adiabatic) and cold ($T_w \sim T_\infty$) wall conditions, since the viscosity depends on temperature. The two ballistic range conditions already discussed fall into the intermediate Reynolds number range, although they appeared to show the high Reynolds number wake behavior. On the other hand, Ragsdale and Darling's[32] measurements in a wind tunnel at $M_\infty = 5$ showed a pronounced

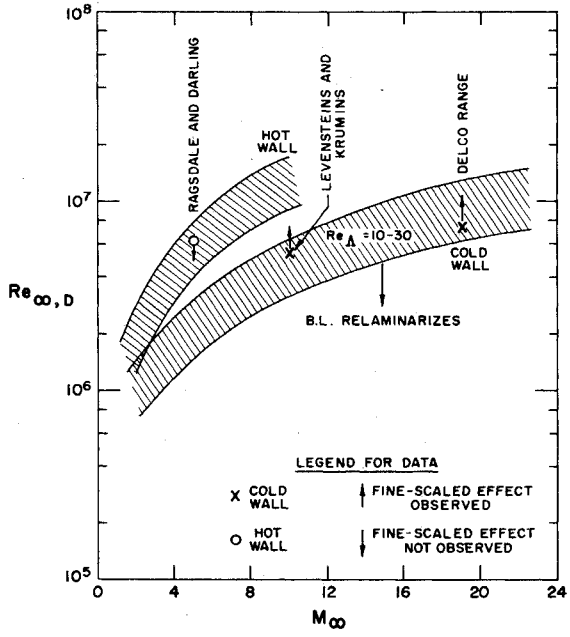

Fig. 10 Predicted conditions for occurrence of fine-scaled near wake turbulence effects.

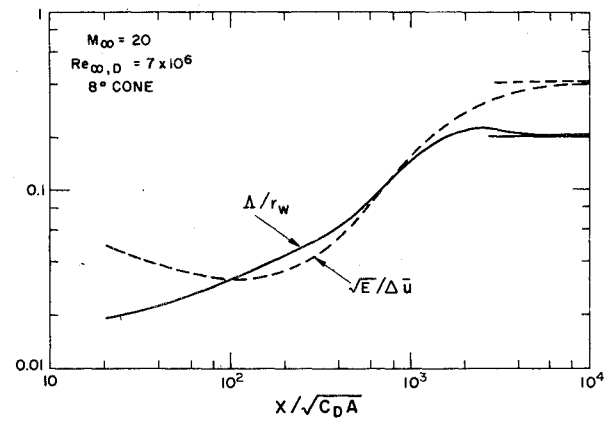

Fig. 11 Computed downstream development of wake axis turbulent intensity and macroscale.

wake growth rate right from the neck. Thus the behavior in their case was probably in the low Reynolds regime, although their conditions also fall in the appropriate intermediate zone. As a result the present data base for cases with turbulent boundary layers does not shed definitive light on the accuracy of the predictions in Fig. 10. Additional tests at other Mach and Reynolds numbers would obviously be of interest.

We now turn to the question of foremost interest—behavior of the wake turbulence downstream of the neck. In particular, what is the distance required for recovery to equilibrium wake turbulence, and can the slow wake growth of the data in Fig. 3 be explained in detail? To this end, we applied an integral method of solution to Eqs. (10–14). These equations are solved simultaneously with the mean flow equations of the Lees-Hromas model, with the obvious difference that the eddy viscosity used in the mean momentum equation is determined from the computed Reynolds stress.

In the integral method, relative radial profiles are specified in terms of the Howarth-Dorodnitsyn radial coordinate for the various turbulent quantities. The partial differential equations are integrated across the wake, yielding ordinary differential equations for the unknown axis values. Integration with respect to downstream distance yields the solution. In our formulation there are eight such equations for the axis values of $\bar{u}$, $\bar{h}$, $\hat{u}_x$, $\hat{u}_r$, $\hat{u}_\theta$, ε (from $\overline{u_x' u_r'}$), and Λ and for r_w. The profiles used were: gaussians for the mean quantities, modified gaussians with a 20% off-axis peak for the fluctuating velocities (obtained by curve-fitting the data of Carmody[9] and Demetriades[10]), a parabola for the eddy viscosity (suggested by Carmody's data[9]), and a uniform profile for Λ. Inasmuch as the resulting expressions are rather intricate and provide no additional insight, they will not be presented here. The integral equations were evaluated in the asymptotic far wake limit to insure that they produce a reasonable description of equilibrium wake turbulence.

There are two noteworthy features which result from the application of an integral method to Eqs. (10–14). First, if one introduces a gradient diffusion model for turbulent diffusion and neglects axial diffusion under the boundary-layer approximation, the turbulent diffusion terms disappear upon integration across the wake. Diffusion terms play an important role in determining the radial profiles but are swept under the rug by an integral approach. Thus our lack of concern above with closure approximations for them. Second, because of symmetry, we must have $\hat{u}_r^2 = \hat{u}_\theta^2$ on the axis. Although there might be some difference in the radial profiles of these two quantities, the difference seems a rather fine point for present purposes and was neglected, with the result that the solutions for $\hat{u}_r^2$ and $\hat{u}_\theta^2$ are identical.

It must be admitted that a certain level of numerical inaccuracy is likely to be introduced by the use of an integral method since similarity of the radial profiles in the near wake cannot be justified. However, any such errors probably are unimportant

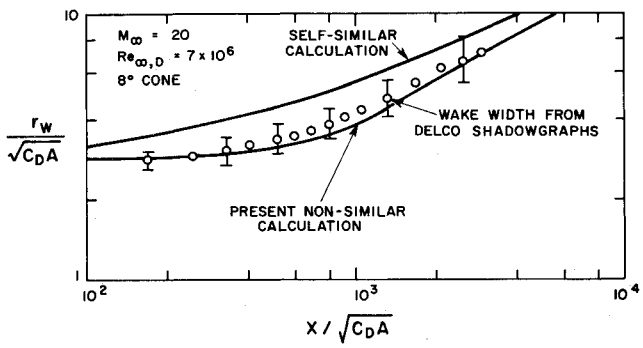

Fig. 12 Comparison of nonsimilar turbulence calculation of wake radius with that measured from Delco shadowgraphs.[5] The self-similar turbulence calculation is shown for reference.

in light of the approximations required for closure and the large departures from equilibrium turbulence levels. Eventual analyses may incorporate finite-difference computations.

Wake computations have been performed for the $M_\infty = 20$ ballistic range conditions appropriate to the turbulent boundary-layer case of Fig. 3. The integral calculations were started at $x/D = 4$ or $x/(C_DA)^{1/2} \cong 20$, where the pressure has relaxed to nearly ambient values. The initial turbulent properties were taken from the streamline computation just described, with a presumption that the values on that streamline are representative of the entire inner portion of the wake. The predicted downstream development of the scale size and axial fluctuation intensity are shown in Fig. 11. Bear in mind that the normalizing quantities r_w and $\Delta\bar{u}$ are nearly constant out to $x/(C_DA)^{1/2} \sim 10^3$. This calculation reflects the fact that dissipation is very important in the near wake, because the scale size is small there. Dissipation causes the scale size to increase and the intensity to decrease initially. Only after the scale size has increased can production of energy overcome dissipation, so the recovery of the turbulent intensity to similarity tends to lag the recovery of the scale size. Complete similarity is not attained until $x/(C_DA)^{1/2} \sim 3000$.

The corresponding solution for the wake growth is shown in Fig. 12. Agreement is seen to be generally good, with the calculation exhibiting perhaps a bit more nonsimilarity than do the shadowgraph data.

V. Conclusions

This study has attempted to describe a rather interesting turbulence phenomenon occurring in high Reynolds number hypersonic wakes. Admittedly, the present results are somewhat speculative. The basic model is based largely upon shadowgraph observations, and it is well-known that shadowgraphs are not always the most reliable source of fluid mechanical data. Nevertheless, the available data seem to indicate quite clearly that existing models do not suffice for high Reynolds number wakes and that such wakes represent a situation where detailed turbulence descriptions are fundamentally necessary. The formulation that has been developed to predict the required turbulence parameters yields a reasonable comparison with the observed wake growth. For the high Reynolds number wake behavior to occur, computations suggest that the Reynolds number should not only be sufficiently large for a well-developed turbulent boundary layer to exist, it should also be high enough for the turbulence not to "relaminarize" during the trailing edge expansion. Much work remains to be done. The idea of computing the detailed behavior of second-order turbulence parameters is quite ambitious and the present approach could undoubtedly be improved, particularly regarding compressibility effects. The nature of the postulated stabilization of the near wake by the residual boundary-layer turbulence is unknown. Finally, it is clear that detailed laboratory measurements of mean and fluctuating properties would be invaluable for confirming the present concept of high Reynolds number wake behavior and for defining the regime where it prevails.

Appendix: Conservation Equation for Scale Size

Rotta[17] has derived a conservation equation for the scale size. However, for high turbulence Reynolds numbers, an equation may be derived in a more positive manner, making direct use of Kolmogorov's universal equilibrium hypothesis (as mentioned in Sec. III, the low Reynolds number case has been solved exactly by Batchelor and Townsend[21]). Several approximations shall be invoked here, most of which were mentioned above: incompressible turbulence, isotropic spectrum (only one scale size Λ), and negligible variation in mean properties over a scale length.

As Rotta showed,[17] the scale size equation results from the conservation equation for the spectrum of the kinetic energy. The spectrum is given by the Fourier transform of the autocorrelation of the kinetic energy

$$F(\mathbf{x},k,t) = \frac{k^2}{2\pi^2}\int_0^\infty R(\mathbf{x},\mathbf{r},t)\frac{\sin kr}{kr}\,d^3\mathbf{r}$$

$$R(\mathbf{x},\mathbf{r},t) = \sum_{i=1}^{3}\overline{u_i'(\mathbf{x},t)u_i'(\mathbf{x}+\mathbf{r},t)} \tag{A1}$$

The kinetic energy and macroscale are related to the spectrum by

$$E(\mathbf{x},t) = \int_0^\infty F(\mathbf{x},k,t)\,dk \tag{A2}$$

$$\Lambda = k_e^{-1} = \frac{6\pi}{8E}\int_0^\infty F(\mathbf{x},k,t)k^{-1}\,dk \tag{A3}$$

As defined here, Λ may be identified with the longitudinal integral scale, often denoted by Λ_f.

The conservation equation for the spectrum is[17]

$$\begin{matrix}\text{(Convection)} & \text{(Production)} & \left\{\begin{matrix}\text{Turbulent} & \text{Diffusion}\\ \text{in } x & \text{in } k\end{matrix}\right\}\end{matrix}$$

$$\bar{\rho}(DF/Dt) = -\bar{\rho}F_{ij}(\partial\bar{u}_i/\partial x_j) + \bar{\rho}\nabla\cdot F_E + \bar{\rho}W$$

$$\begin{matrix}\text{(Molecular)}\\ \text{Diffusion}\end{matrix}\quad\begin{matrix}\text{(Dissipation)}\\ \end{matrix}$$

$$+\tfrac{1}{2}\mu\nabla^2F - 2\mu k^2F \tag{A4}$$

Here, F_{ij} is the transform of the Reynolds stress, and F_E and W come from the turbulent energy diffusion (triple velocity fluctuation) terms. As we shall be interested only in an average value of the spectrum or macroscale at a given station in a wake, we will disregard the spatial diffusion terms. The problem terms in Eq. (A4) are F_{ij} and the transfer spectrum (cascade term) $W(k)$. To describe these terms we take advantage of Kolmogorov's universal equilibrium hypothesis, as a result of the large separation between dissipation and energy-containing wave numbers, and invoke similarity for spectral shapes. We can define a wave number k^*, below which all the energy exists and dissipation is negligible, and above which only the dissipation and cascade terms are important. Thus, with Φ the dissipation rate

$$\int_{k*}^\infty W(k)\,dk = \int_{k*}^\infty 2\nu k^2F(k)\,dk = \Phi$$

Since

$$\int_0^\infty W(k)\,dk = 0, \qquad \int_0^{k*} W(k)\,dk = -\Phi$$

If we assume spectral similarity and that the spectral shape for $k \lesssim k^*$ depends only on the energy-containing wave number,

$$W(k) = -1/c_1(1/k_e)\Phi g_1(k/k_e) \quad \text{for} \quad k \lesssim k^* \tag{A5}$$

Similarly, for F_{ij},

$$F_{ij}(k) = +\frac{1}{c_2}\frac{1}{k_e}\overline{u_i'u_j'}\,g_2(k/k_e) \quad \text{for} \quad k \lesssim k^* \tag{A6}$$

where

$$c_{1,2} = \int_0^{k*} g_{1,2}(k/k_e)\, d(k/k_e)$$

Insertion of Eqs. (A5) and (A6) into Eq. (A4) and integration from 0 to k^* give the familiar turbulent kinetic energy equation

$$\bar{\rho}\frac{DE}{Dt} = -\bar{\rho}\,\overline{u_i'u_j'}\frac{\partial \bar{u}_i}{\partial x_j} - \bar{\rho}\Phi + (\text{Diffusion terms}) \qquad \text{(A7)}$$

Multiplication by k^{-1} and integration from 0 to k^* yields

$$\rho\, D(E\Lambda)/Dt = -\bar{\rho}\,\overline{u_i'u_j'}(\partial \bar{u}_i/\partial x_j)\Lambda d_2 - \bar{\rho}\Phi\Lambda\, d_1 + (\text{Diffusion terms}) \qquad \text{(A8)}$$

where

$$d_{1,2} = \frac{6\pi}{8c_{1,2}}\int_0^{k*} g_{1,2}(k/k_e)(k/k_e)^{-1} d\left(\frac{k}{k_e}\right)$$

are supposedly universal "closure" constants.

Subtraction of Eq. (A7) from Eq. (A8) yields the expression cited in Sec. III in the $Re_\Lambda \to \infty$ limit. For finite turbulence Reynolds numbers we must include an additional term. Following Batchelor and Townsend's[21] work on low Reynolds number turbulence, the required term in Eq. (A8) is $\pi\mu E/\Lambda$, or $\pi\mu/\Lambda$ in Eq. (14).

References

[1] Lees, L. and Hromas, L., "Turbulent Diffusion in the Wake of a Blunt-Nosed Body at Hypersonic Speeds," *Journal of Aerospace Sciences*, Vol. 29, No. 8, Aug. 1962, pp. 976–992.

[2] Levensteins, Z. J., private communication, 1970, U.S. Naval Ordnance Lab., Silver Spring, Md.

[3] Levensteins, Z. J. and Krumins, M. V., "Aerodynamic Characteristics of Hypersonic Wakes," *AIAA Journal*, Vol. 5, No. 9, Sept. 1967, pp. 1596–1602.

[4] Liquornik, D., private communication, 1971, Delco Electronics, Santa Barbara, Calif.

[5] Shaw, G. A., private communication, 1971, Delco Electronics, Santa Barbara, Calif.

[6] Pirri, A. N., "Decay of Boundary-Layer Turbulence in Near Wake of a Slender Body," *AIAA Journal*, Vol. 10, No. 5, May 1972, pp. 657–663.

[7] Laderman, A. J. and Demetriades, A., "Measurements of the Mean and Turbulent Flow in a Cooled-Wall Boundary Layer at Mach 9.37," AIAA Paper 72-73, San Diego, Calif., 1972.

[8] Townsend, A. A., *The Structure of Turbulent Shear Flow*, Cambridge University Press, Cambridge, England, 1956, Chap. 7.

[9] Carmody, T., "Establishment of the Wake Behind a Disk," *Journal of Basic Engineering*, Vol. 86, No. 4, Dec. 1964, pp. 869–882.

[10] Demetriades, A., "Turbulence Measurements in an Axisymmetric Compressible Wake," *Physics of Fluids*, Vol. 11, No. 9, Sept. 1968, pp. 1841–1852.

[11] Hinze, J. O., *Turbulence*, McGraw-Hill, New York, 1959, p. 48.

[12] Lees, L., "Hypersonic Wakes and Trails," *AIAA Journal*, Vol. 2, No. 3, March 1964, pp. 417–428.

[13] Crow, S. C., "Viscoelastic properties of fine-grained incompressible turbulence," *Journal of Fluid Mechanics*, Vol. 33, Pt. 1, July 1968, pp. 1–20.

[14] Crow, S. C. and Champagne, F. H., "Orderly structure in jet turbulence," *Journal of Fluid Mechanics*, Vol. 48, Pt. 3, Aug. 1971, pp. 547–592.

[15] Roshko, A., "On the Development of Turbulent Wakes from Vortex Streets," Rept. 1191, 1954, NACA.

[16] Bradshaw, P. and Wong, F. Y. F., "The reattachment and relaxation of a turbulent shear layer," *Journal of Fluid Mechanics*, Vol. 52, Pt. 1, March 1972, pp. 113–135.

[17] Rotta, J., "Statistische Theorie nichthomogener Turbulenz," *Zeitschrift für Physik*, Vol. 129, 1951, pp. 547–572, and Vol. 131, 1951, pp. 51–77.

[18] Donaldson, C. duP. and Rosenbaum, H., "Calculation of Turbulent Shear Flows Through Closure of the Reynolds Equations by Invariant Modeling," *Compressible Turbulent Boundary Layers*, NASA SP-216, 1969, pp. 231–253.

[19] Daly, B. J. and Harlow, F. H., "Transport Equations in Turbulence," *Physics of Fluids*, Vol. 13, No. 11, Nov. 1970, pp. 2634–2649.

[20] Hanjalić, K. and Launder, B. E., "A Reynolds stress model of turbulence and its application to thin shear flows," *Journal of Fluid Mechanics*, Vol. 52, Pt. 4, April 1972, pp. 609–638.

[21] Batchelor, G. K. and Townsend, A. A., "Decay of turbulence in the final period," *Proceedings of the Royal Society of London, Series A*, Vol. 194, Nov. 1948, pp. 527–543.

[22] Comte-Bellot, G. and Corrsin, S., "The use of a contraction to improve the isotropy of grid-generated turbulence," *Journal of Fluid Mechanics*, Vol. 25, Pt. 4, Aug. 1966, pp. 657–682.

[23] Comte-Bellot, G. and Corrsin, S., "Simple Eulerian time correlation of full- and narrow-band velocity signals in grid-generated 'isotropic' turbulence," *Journal of Fluid Mechanics*, Vol. 48, Pt. 2, July 1971, pp. 273–337.

[24] Batchelor, G. K. and Townsend, A. A., "Decay of isotropic turbulence in the initial period," *Proceedings of the Royal Society of London*, Ser. A, Vol. 193, July 1948, pp. 539–558.

[25] Uberoi, M. S., "Energy Transfer in Isotropic Turbulence," *Physics of Fluids*, Vol. 6, No. 8, Aug. 1963, pp. 1048–1056.

[26] Kistler, A. L. and Vrebalovich, T., "Grid turbulence at large Reynolds numbers," *Journal of Fluid Mechanics*, Vol. 26, Pt. 1, Sept. 1966, pp. 37–47.

[27] Champagne, F. H., Harris, V. G., and Corrsin, S., "Experiments on nearly homogeneous turbulent shear flow," *Journal of Fluid Mechanics*, Vol. 41, Pt. 1, March 1970, pp. 81–139.

[28] Rose, W. G., "Results of an attempt to generate a homogeneous turbulent shear flow," *Journal of Fluid Mechanics*, Vol. 25, Pt. 1, May 1966, pp. 97–120.

[29] Finson, M. L. and Weiss, R. F., "A Theoretical Investigation of the Hypersonic Axisymmetric Near Wake Recompression Region," RR 334, July 1969, Avco Everett Research Lab., Everett, Mass.

[30] Demetriades, A., private communication, 1972, Philco-Ford Corp., Newport Beach, Calif.

[31] Maise, G. and McDonald, H., "Mixing Length and Kinematic Eddy Viscosity in a Compressible Boundary Layer," *AIAA Journal*, Vol. 6, No. 1, Jan. 1968, pp. 73–80.

[32] Ragsdale, W. C. and Darling, J. A., "An Experimental Study of the Turbulent Wake Behind a Cone at $M = 5$," *Proceedings of the 1966 Heat Transfer and Fluid Mechanics Institute*, Stanford University Press, Stanford, Calif., 1966, pp. 198–209.